

Short-range correlation physics at low RG resolution

Anthony Tropiano¹, Scott Bogner², Dick Furnstahl¹

¹Ohio State University, ²Michigan State University

APS DNP Meeting – Virtual Meeting

October 12, 2021

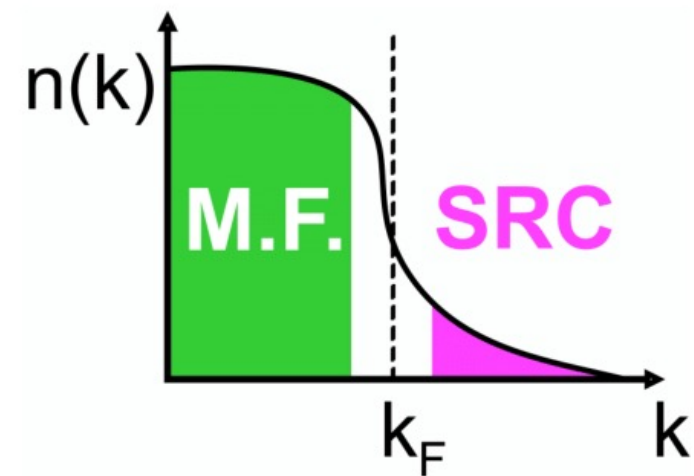
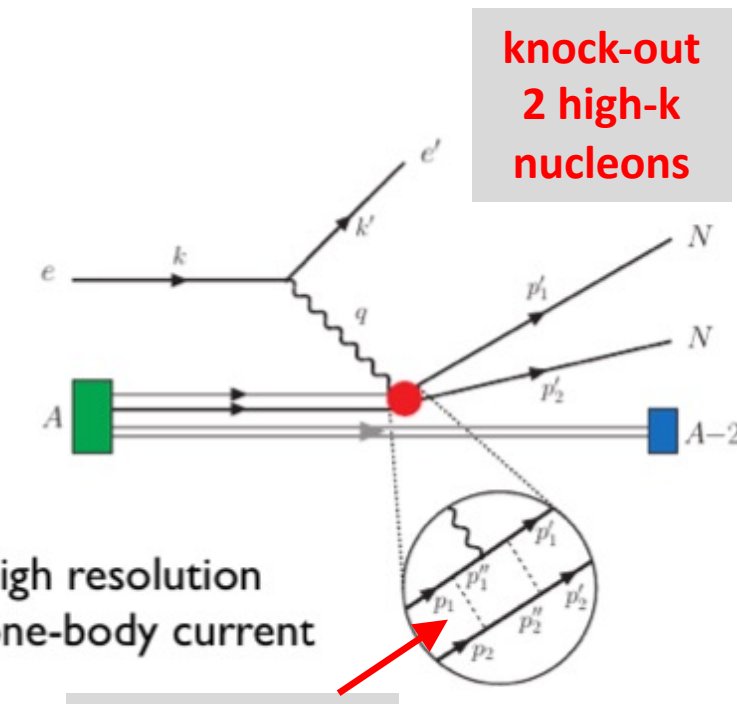
ajt, S.K. Bogner, and R.J. Furnstahl, arXiv:2105.13936

*Phys. Rev. C **104**, 034311 (2021)*



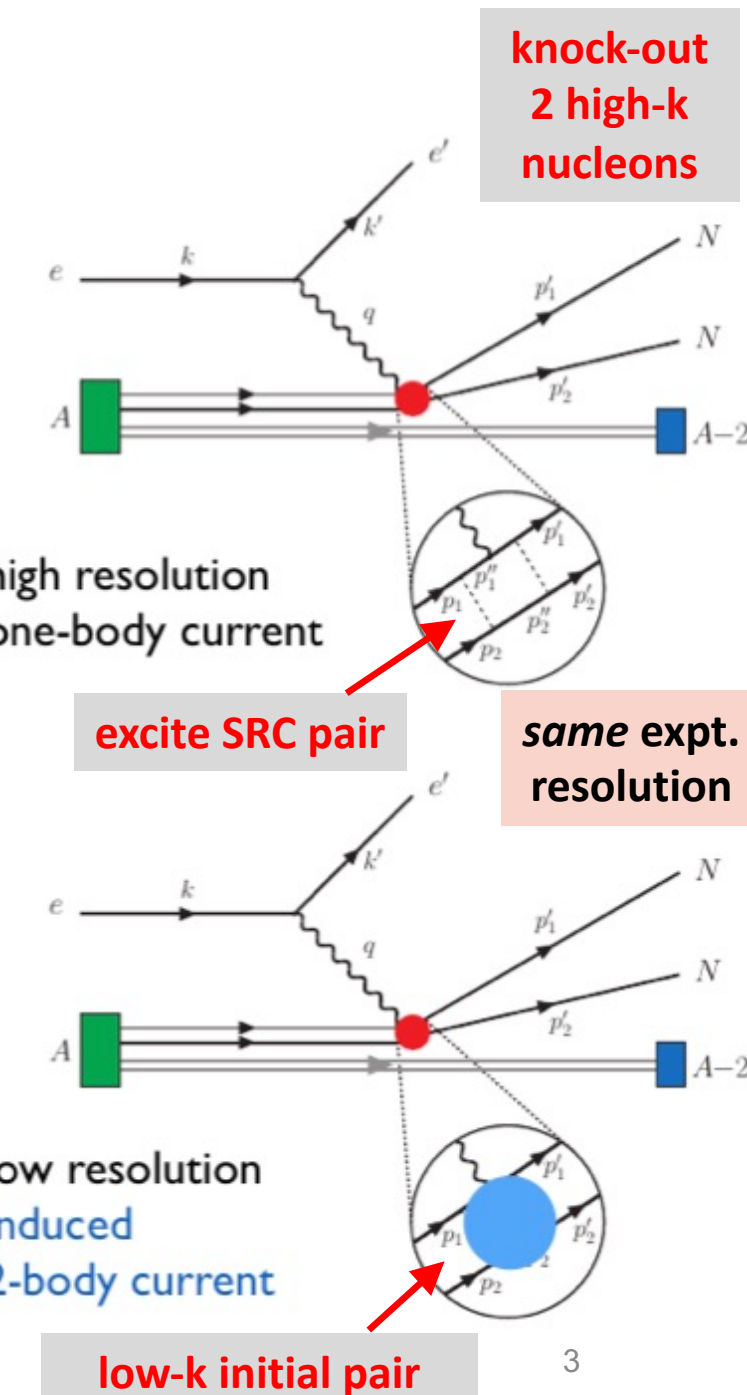
Motivation

- Recent experiments have been able to isolate processes where short-range correlation (SRC) physics is dominant and well accounted for by SRC phenomenology
- SRC physics at **high RG resolution**
 - SRC pairs are components in the nuclear wave function with relative momenta above the Fermi momentum



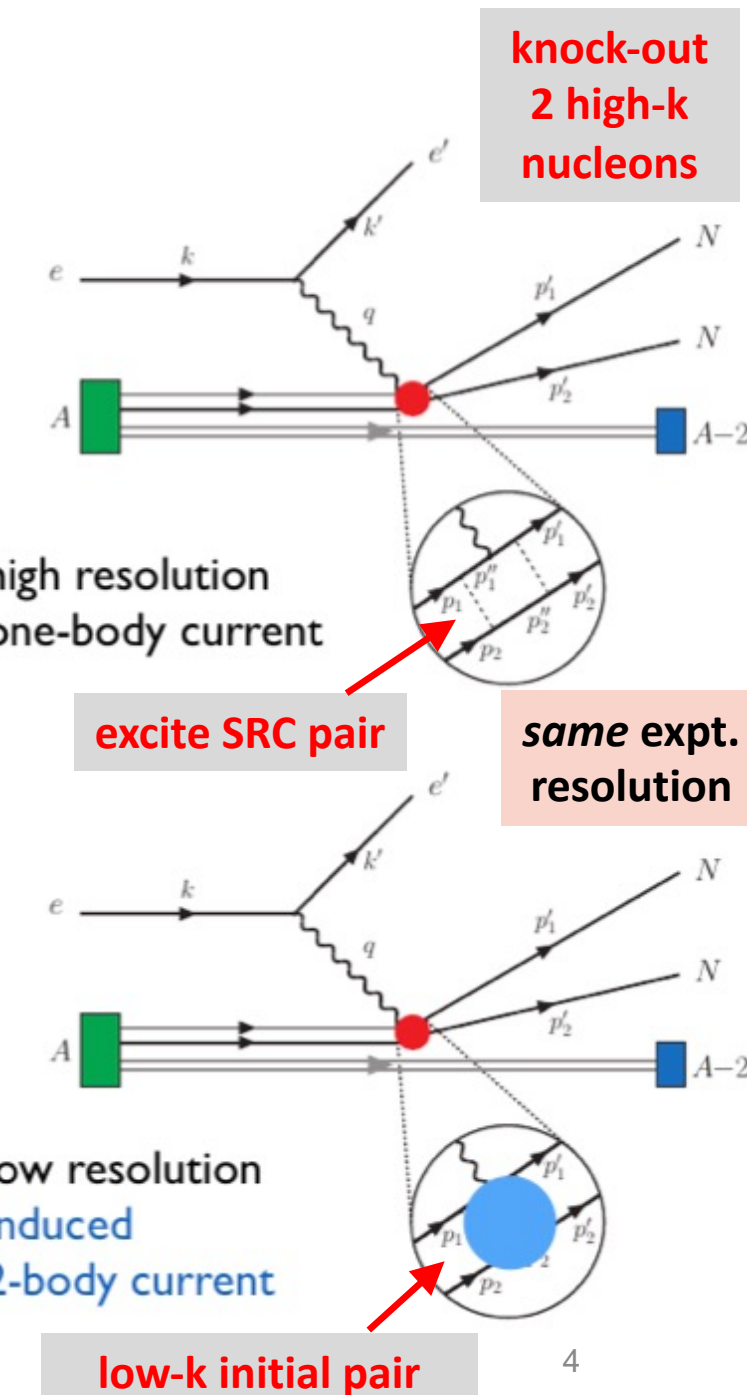
Motivation

- Recent experiments have been able to isolate processes where short-range correlation (SRC) physics is dominant and well accounted for by SRC phenomenology
- SRC physics at **low RG resolution**
 - The SRC *physics* is shifted into the reaction operators from the nuclear wave function (which becomes soft)
 - Operators do not become hard, which simplifies calculations



Motivation

- Recent experiments have been able to isolate processes where short-range correlation (SRC) physics is dominant and well accounted for by SRC phenomenology
- SRC physics at **low RG resolution**
 - The SRC *physics* is shifted into the reaction operators from the nuclear wave function (which becomes soft)
 - Operators do not become hard, which simplifies calculations
- Experimental resolution (set by momentum of probe) is the same in both pictures**
- Same observables but different physical interpretation!**



Similarity Renormalization Group (SRG)

- AV18 wave function has significant SRC
- What happens to the wave function at low RG resolution?
- Use SRG to unitarily evolve to low RG resolution where λ gives the decoupling scale

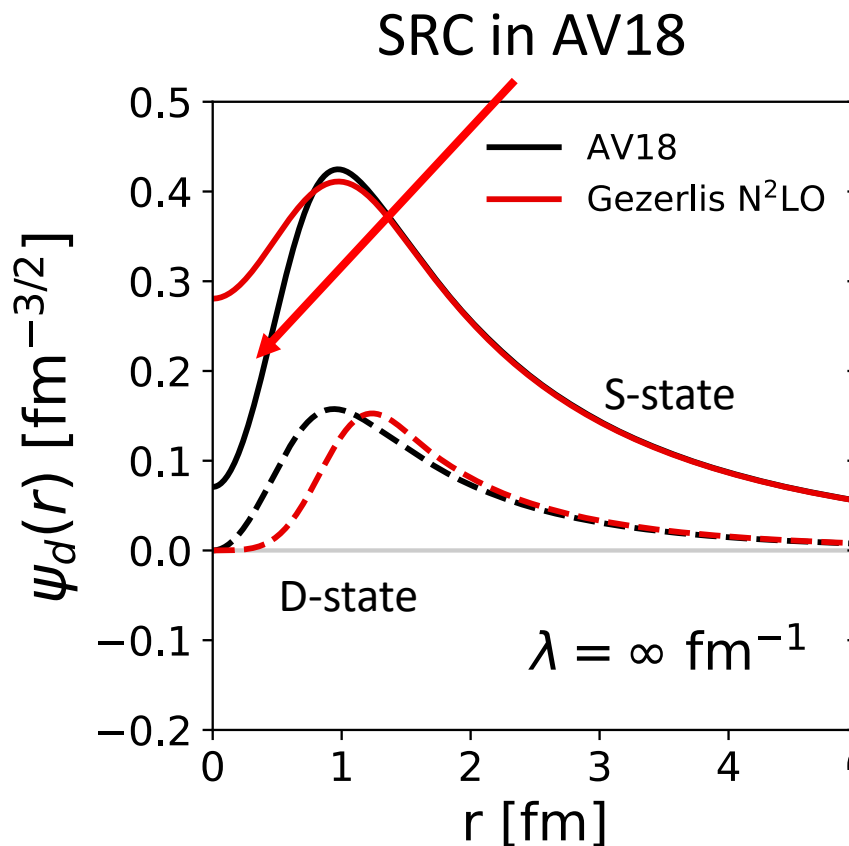


Fig. 1: SRG evolution of deuteron wave function in coordinate space for AV18 and Gezerlis N²LO¹.

Similarity Renormalization Group (SRG)

- SRC physics in AV18 is gone from wave function at low RG resolution
- Deuteron wave functions become soft and D-state probability goes down
- Observables such as asymptotic D-S ratio are the same

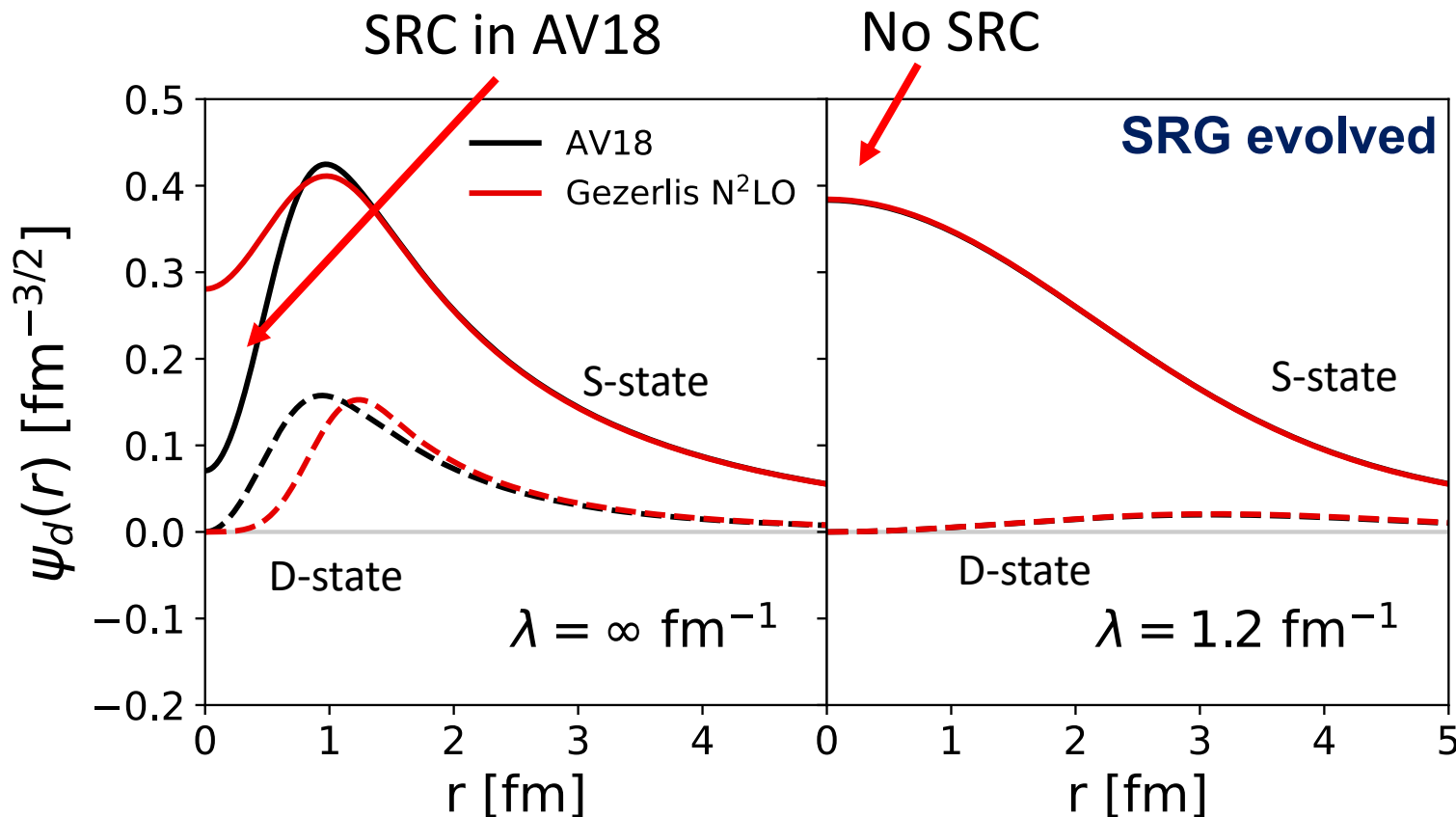


Fig. 1: SRG evolution of deuteron wave function in coordinate space for AV18 and Gezerlis N²LO¹.

Momentum distributions at low RG resolution

- Soft wave functions at low RG resolution
 - Where does the SRC physics go?

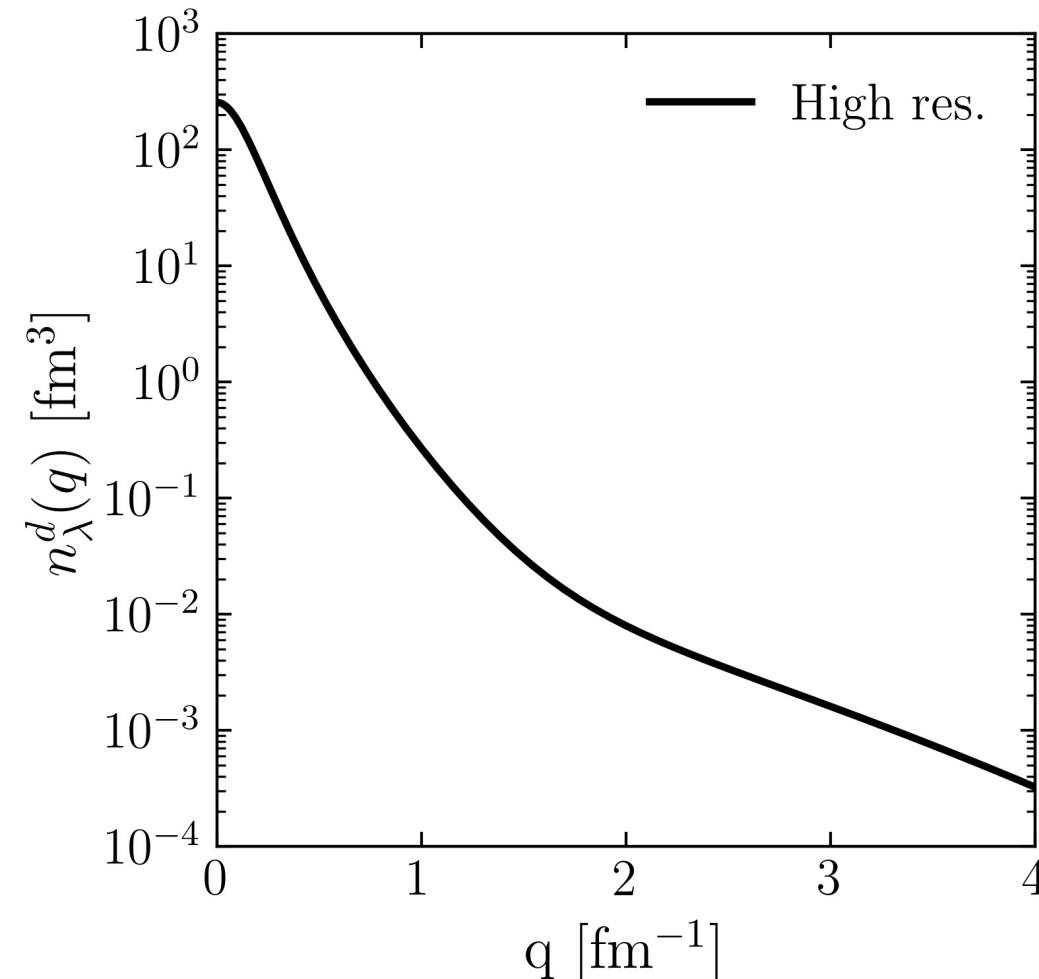
Momentum distributions at low RG resolution

- Soft wave functions at low RG resolution
 - Where does the SRC physics go?
- SRC physics shifts to the operators $\langle \psi_f^{hi} | U_\lambda^\dagger U_\lambda O^{hi} U_\lambda^\dagger U_\lambda | \psi_i^{hi} \rangle$
- Apply SRG transformations to momentum distribution operator

$$n^{hi}(\mathbf{q}) = a_{\mathbf{q}}^\dagger a_{\mathbf{q}}$$

$$U_\lambda = 1 + \frac{1}{4} \sum_{K, \mathbf{k}, \mathbf{k}'} \delta U_\lambda^{(2)}(\mathbf{k}, \mathbf{k}') a_{\frac{K}{2}+\mathbf{k}}^\dagger a_{\frac{K}{2}-\mathbf{k}}^\dagger a_{\frac{K}{2}-\mathbf{k}'} a_{\frac{K}{2}+\mathbf{k}'} + \dots$$

Momentum distributions at low RG resolution



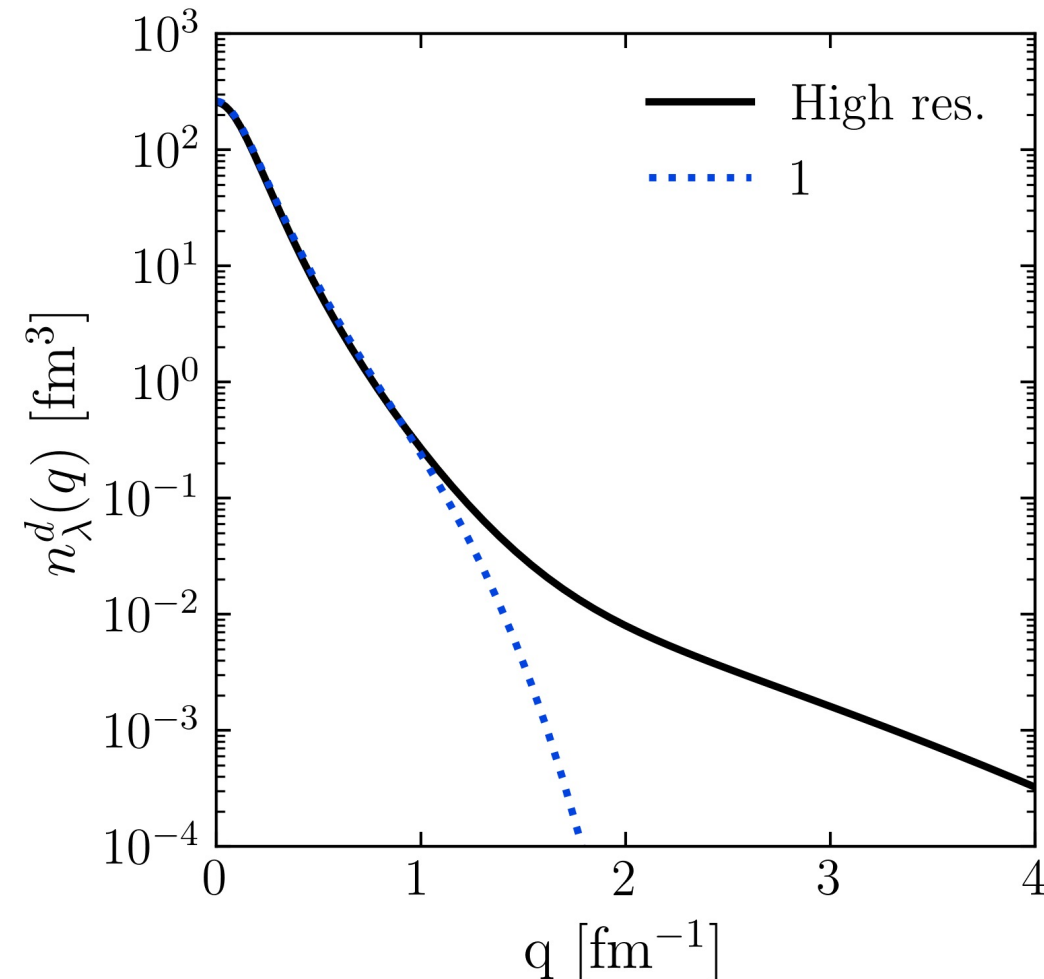
- Deuteron example

$$n^{lo}(\mathbf{q}) = (1 + \delta U) a_{\mathbf{q}}^\dagger a_{\mathbf{q}} (1 + \delta U^\dagger)$$

$$\langle \psi_d^{hi} | a_{\mathbf{q}}^\dagger a_{\mathbf{q}} | \psi_d^{hi} \rangle$$

Fig. 2: Contributions to deuteron momentum distribution with AV18 and $\lambda = 1.35$ fm⁻¹.

Momentum distributions at low RG resolution



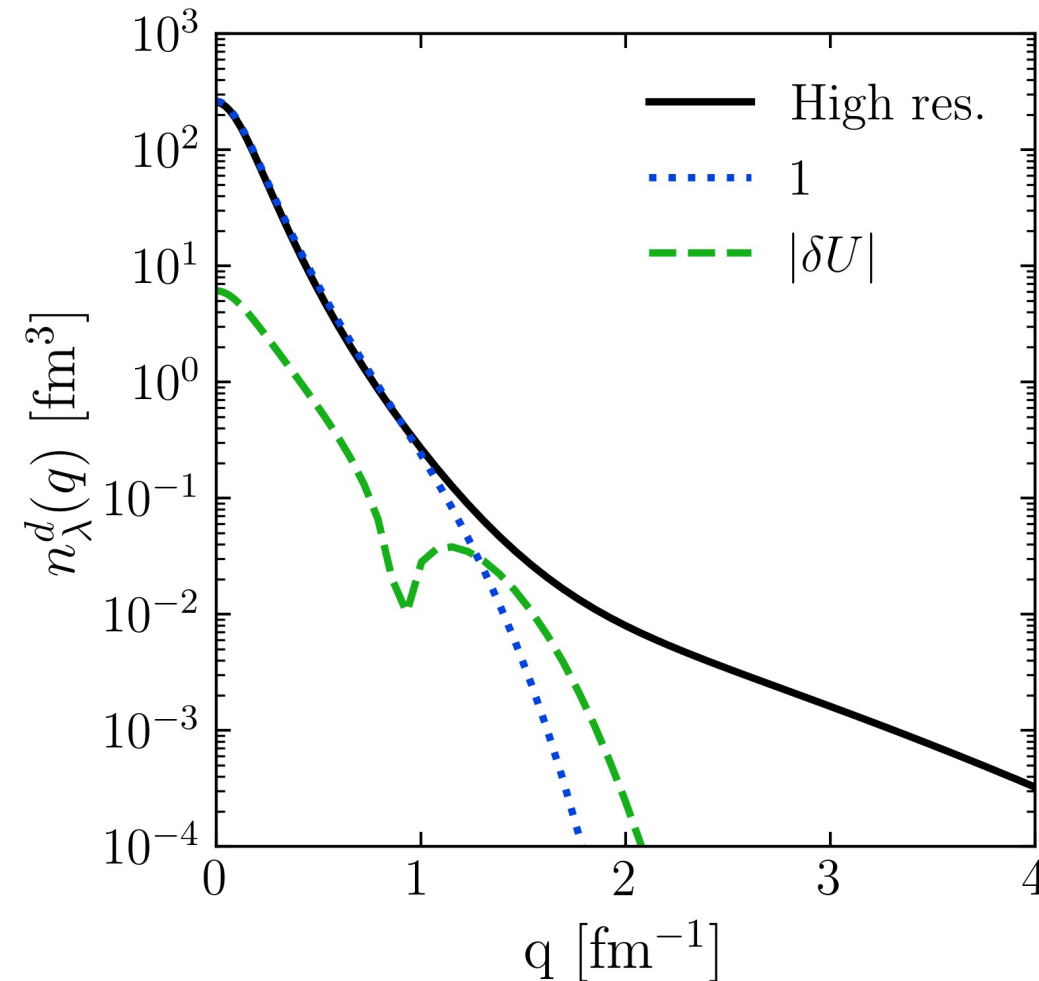
- Deuteron example

$$n^{lo}(\mathbf{q}) = (1 + \delta U) a_{\mathbf{q}}^\dagger a_{\mathbf{q}} (1 + \delta U^\dagger)$$

$$\begin{aligned}\langle \psi_d^{hi} | a_{\mathbf{q}}^\dagger a_{\mathbf{q}} | \psi_d^{hi} \rangle \\ \langle \psi_d^{lo} | a_{\mathbf{q}}^\dagger a_{\mathbf{q}} | \psi_d^{lo} \rangle\end{aligned}$$

Fig. 2: Contributions to deuteron momentum distribution with AV18 and $\lambda = 1.35$ fm⁻¹.

Momentum distributions at low RG resolution



- Deuteron example

$$n^{lo}(\mathbf{q}) = (1 + \delta U) a_{\mathbf{q}}^\dagger a_{\mathbf{q}} (1 + \delta U^\dagger)$$

$$\langle \psi_d^{hi} | a_{\mathbf{q}}^\dagger a_{\mathbf{q}} | \psi_d^{hi} \rangle$$

$$\langle \psi_d^{lo} | a_{\mathbf{q}}^\dagger a_{\mathbf{q}} | \psi_d^{lo} \rangle$$

$$\langle \psi_d^{lo} | \delta U a_{\mathbf{q}}^\dagger a_{\mathbf{q}} + a_{\mathbf{q}}^\dagger a_{\mathbf{q}} \delta U^\dagger | \psi_d^{lo} \rangle$$

Fig. 2: Contributions to deuteron momentum distribution with AV18 and $\lambda = 1.35$ fm⁻¹.

Momentum distributions at low RG resolution

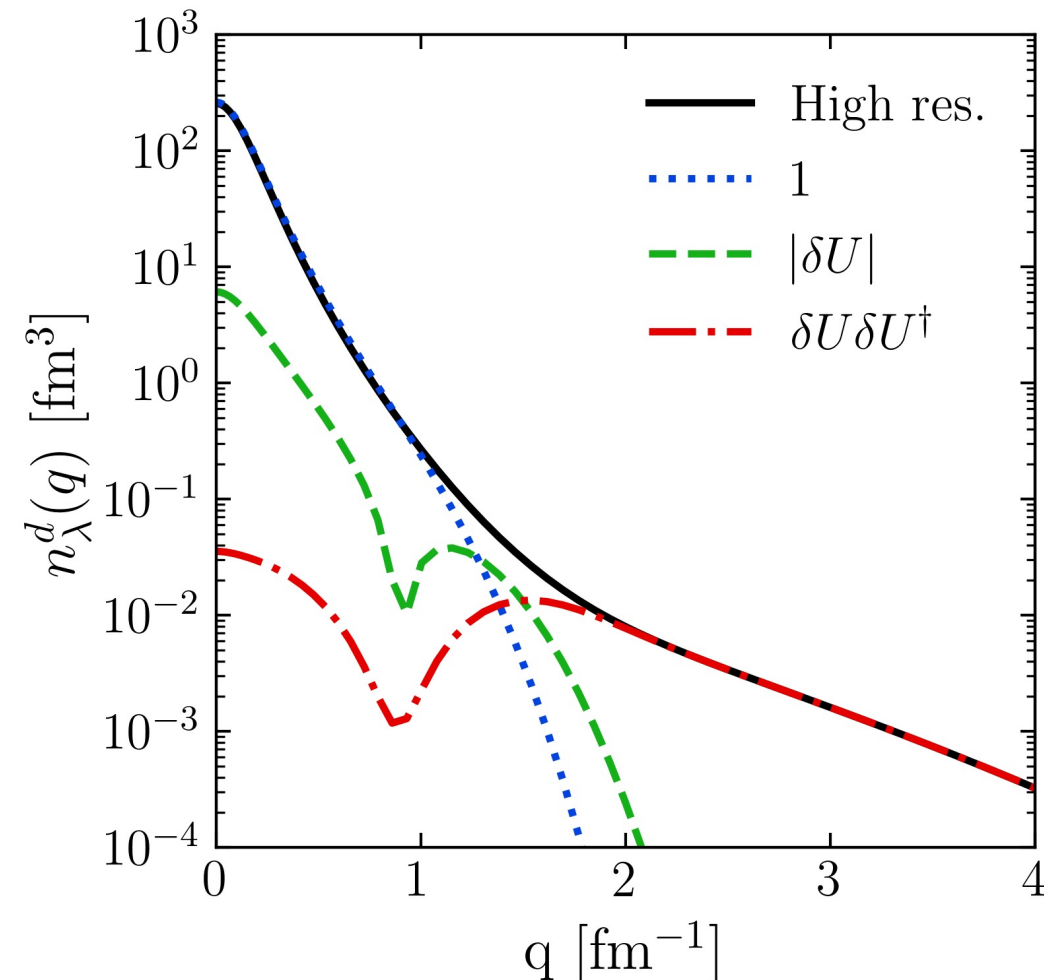


Fig. 2: Contributions to deuteron momentum distribution with AV18 and $\lambda = 1.35 \text{ fm}^{-1}$.

- Deuteron example

$$n^{lo}(\mathbf{q}) = (1 + \delta U) a_{\mathbf{q}}^\dagger a_{\mathbf{q}} (1 + \delta U^\dagger)$$

$$\langle \psi_d^{hi} | a_{\mathbf{q}}^\dagger a_{\mathbf{q}} | \psi_d^{hi} \rangle$$

$$\langle \psi_d^{lo} | a_{\mathbf{q}}^\dagger a_{\mathbf{q}} | \psi_d^{lo} \rangle$$

$$\langle \psi_d^{lo} | \delta U a_{\mathbf{q}}^\dagger a_{\mathbf{q}} + a_{\mathbf{q}}^\dagger a_{\mathbf{q}} \delta U^\dagger | \psi_d^{lo} \rangle$$

$$\langle \psi_d^{lo} | \delta U a_{\mathbf{q}}^\dagger a_{\mathbf{q}} \delta U^\dagger | \psi_d^{lo} \rangle$$

Momentum distributions at low RG resolution

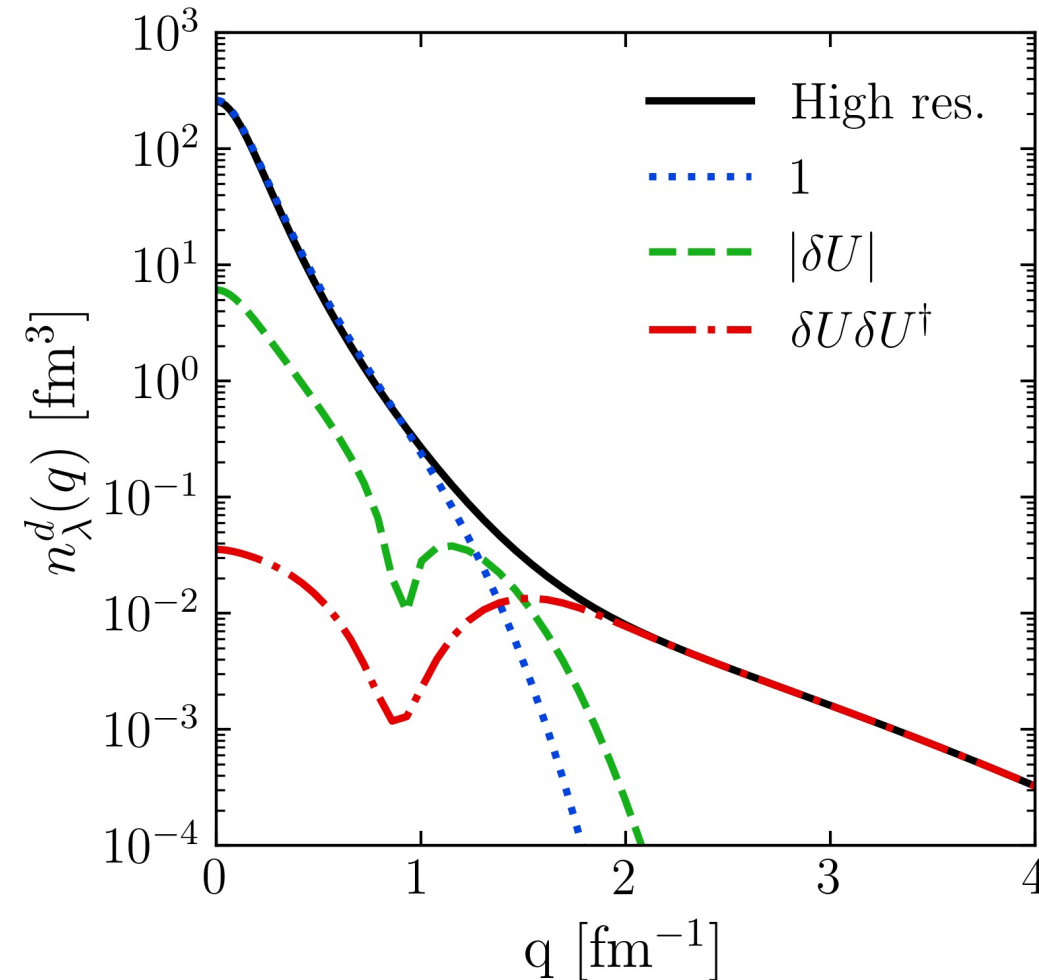
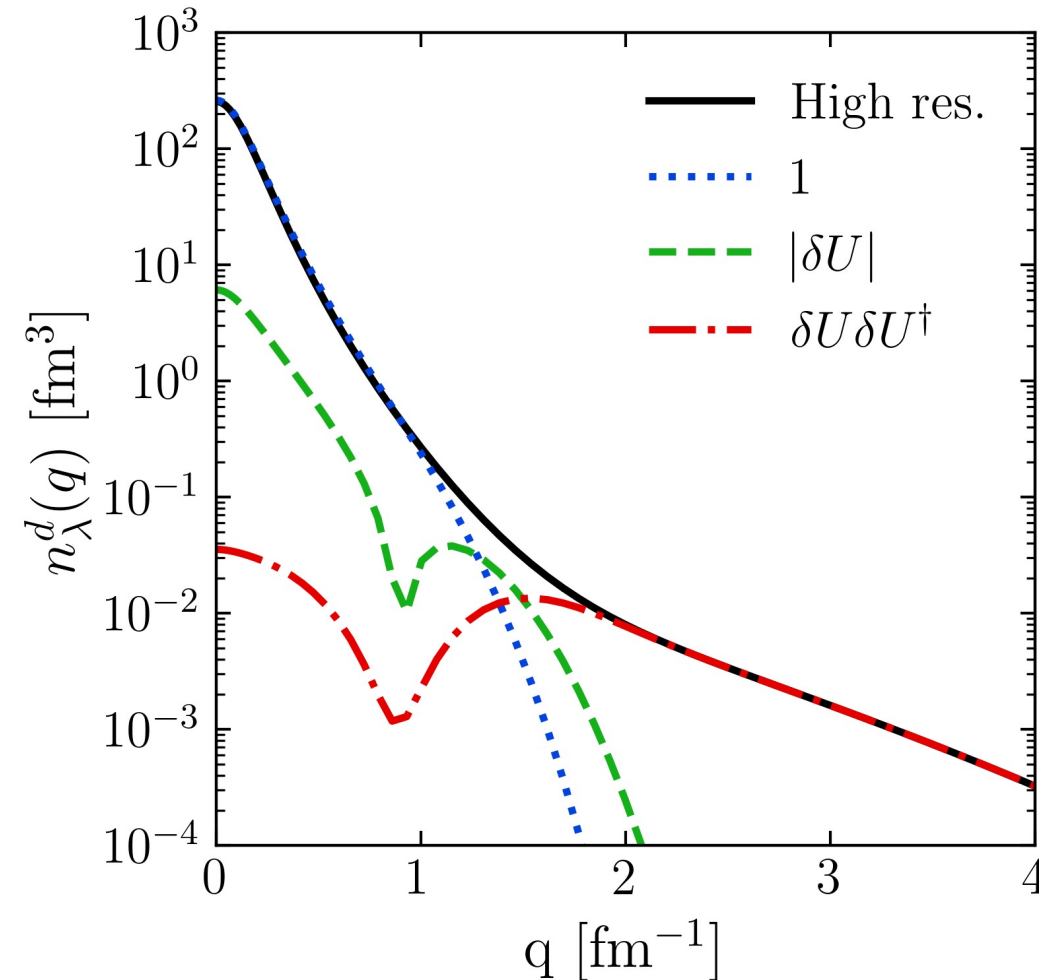


Fig. 2: Contributions to deuteron momentum distribution with AV18 and $\lambda = 1.35 \text{ fm}^{-1}$.

- For high- q , the $\delta U_\lambda \delta U_\lambda^\dagger$ 2-body term dominates

$$\approx \sum_{K,k,k'} \delta U_\lambda(\mathbf{k}, \mathbf{q}) \delta U_\lambda^\dagger(\mathbf{q}, \mathbf{k}') a_{\frac{\mathbf{K}}{2}+\mathbf{k}}^\dagger a_{\frac{\mathbf{K}}{2}-\mathbf{k}}^\dagger a_{\frac{\mathbf{K}}{2}-\mathbf{k}'} a_{\frac{\mathbf{K}}{2}+\mathbf{k}'}$$

Momentum distributions at low RG resolution



- For high- q , the $\delta U_\lambda \delta U_\lambda^\dagger$ 2-body term dominates

$$\approx \sum_{\mathbf{K}, \mathbf{k}, \mathbf{k}'} \delta U_\lambda(\mathbf{k}, \mathbf{q}) \delta U_\lambda^\dagger(\mathbf{q}, \mathbf{k}') a_{\frac{\mathbf{K}}{2} + \mathbf{k}}^\dagger a_{\frac{\mathbf{K}}{2} - \mathbf{k}}^\dagger a_{\frac{\mathbf{K}}{2} - \mathbf{k}'} a_{\frac{\mathbf{K}}{2} + \mathbf{k}'}$$



Factorization: $\delta U_\lambda(\mathbf{k}, \mathbf{q}) \approx F_\lambda^{lo}(\mathbf{k}) F_\lambda^{hi}(\mathbf{q})$

$$\approx |F_\lambda^{hi}(\mathbf{q})|^2 \sum_{\mathbf{K}, \mathbf{k}, \mathbf{k}'}^{\lambda} F_\lambda^{lo}(\mathbf{k}) F_\lambda^{lo}(\mathbf{k}') a_{\frac{\mathbf{K}}{2} + \mathbf{k}}^\dagger a_{\frac{\mathbf{K}}{2} - \mathbf{k}}^\dagger a_{\frac{\mathbf{K}}{2} - \mathbf{k}'} a_{\frac{\mathbf{K}}{2} + \mathbf{k}'}$$

Fig. 2: Contributions to deuteron momentum distribution with AV18 and $\lambda = 1.35$ fm⁻¹.

Momentum distributions at low RG resolution

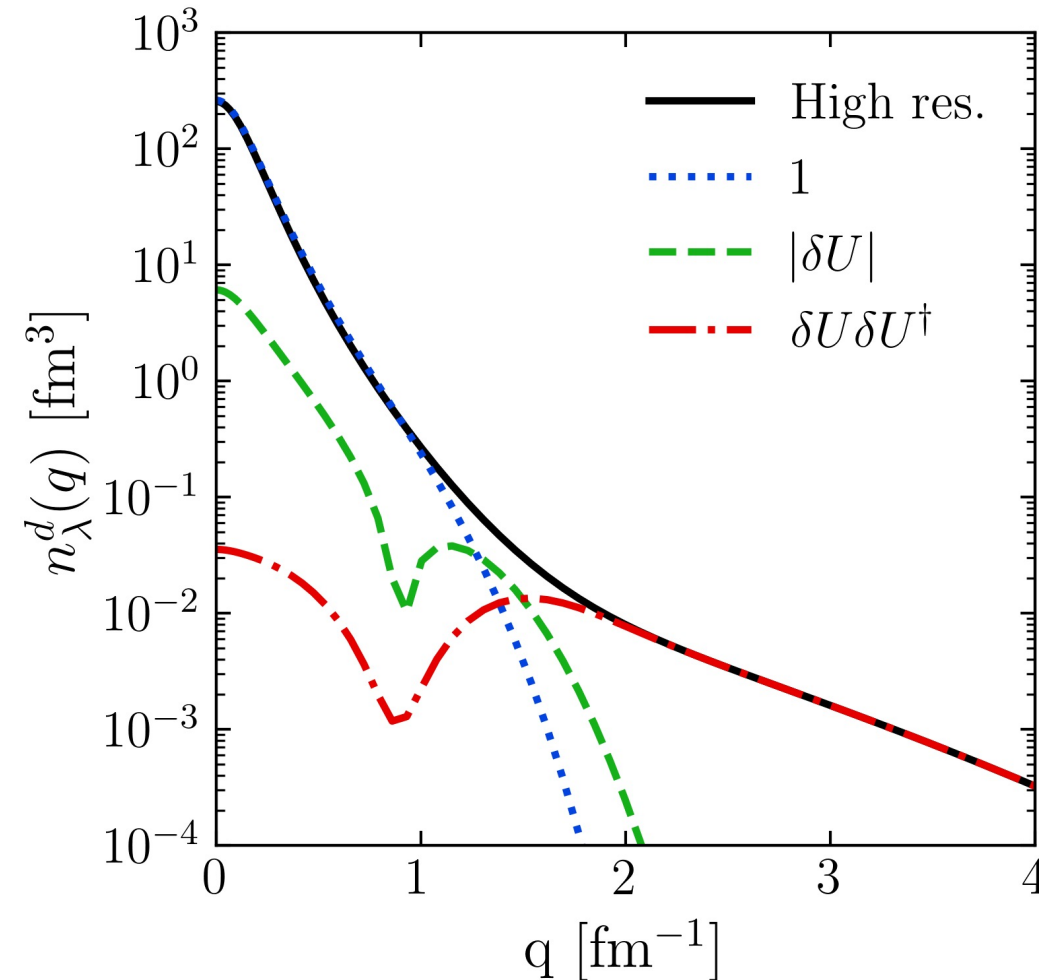


Fig. 2: Contributions to deuteron momentum distribution with AV18 and $\lambda = 1.35 \text{ fm}^{-1}$.

- For high- q , the $\delta U_\lambda \delta U_\lambda^\dagger$ 2-body term dominates

$$\approx \sum \delta U_\lambda(k, q) \delta U_\lambda^\dagger(q, k') a_{\frac{K}{2}+k}^\dagger a_{\frac{K}{2}-k}^\dagger a_{\frac{K}{2}-k'} a_{\frac{K}{2}+k'}$$

Apply this strategy to nuclear momentum distributions using local density approximation (LDA)!

$$\approx |F_\lambda^{lo}(q)|^2 \sum_{K,k,k'} F_\lambda^{lo}(k) F_\lambda^{lo}(k') a_{\frac{K}{2}+k}^\dagger a_{\frac{K}{2}-k}^\dagger a_{\frac{K}{2}-k'} a_{\frac{K}{2}+k'}$$

$$F_\lambda^{hi}(q)$$

Proton momentum distributions

- Low RG resolution calculations reproduce momentum distributions of AV18 data¹ (high RG resolution calculation)

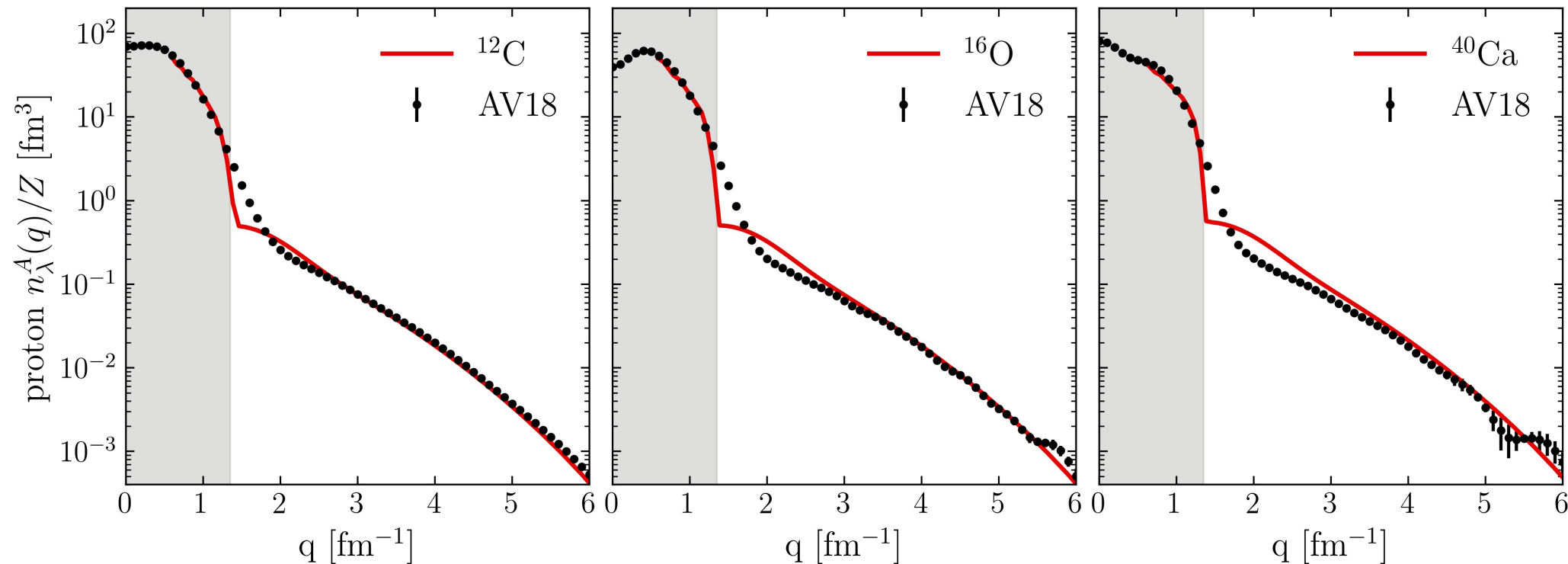


Fig. 3: Proton momentum distributions for ¹²C, ¹⁶O, and ⁴⁰Ca under LDA with AV18, $\lambda = 1.35$ fm⁻¹, and densities from Skyrme EDF SLy4 using the HFBRAD code².

Proton momentum distributions

- **Universality:** High- q dependence from universal function $\approx |F_\lambda^{hi}(q)|^2$ fixed by 2-body and insensitive to nucleus

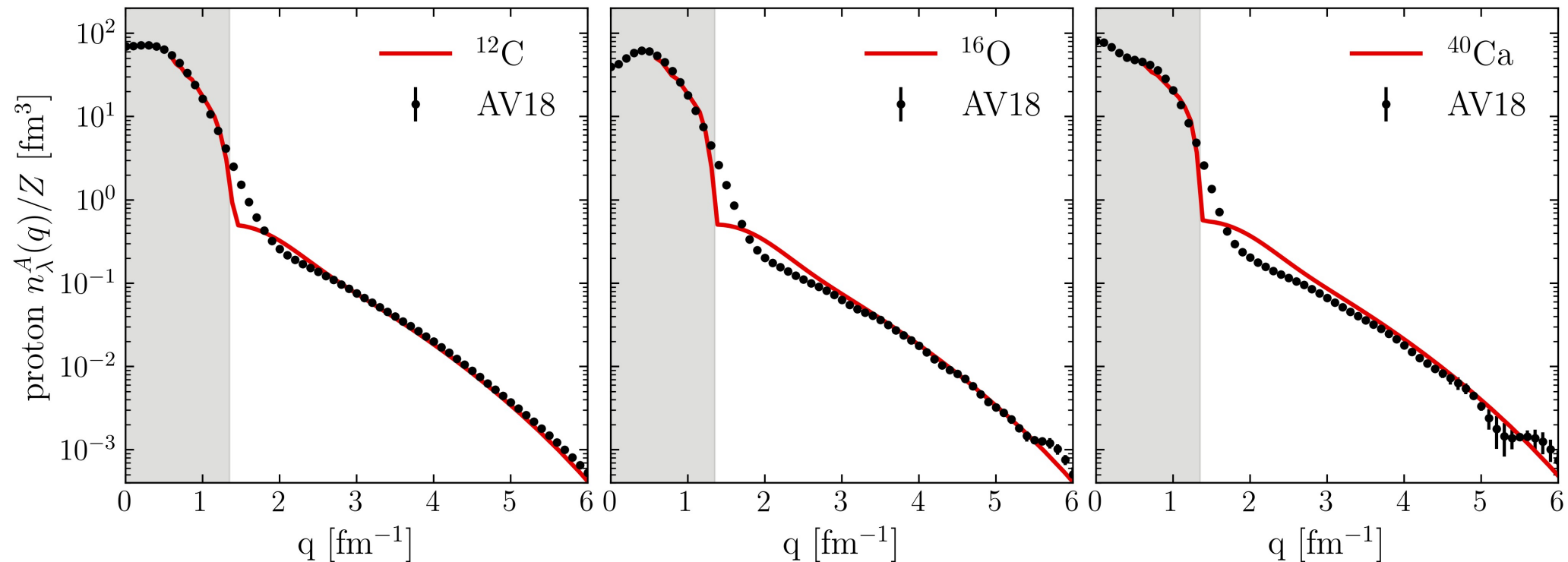


Fig. 3: Proton momentum distributions for ^{12}C , ^{16}O , and ^{40}Ca under LDA with AV18, $\lambda = 1.35$ fm⁻¹, and densities from Skyrme EDF SLy4 using the HFBRAD code².

Proton momentum distributions

- **Universality:** High- q dependence from universal function $\approx |F_\lambda^{hi}(q)|^2$ fixed by 2-body and insensitive to nucleus

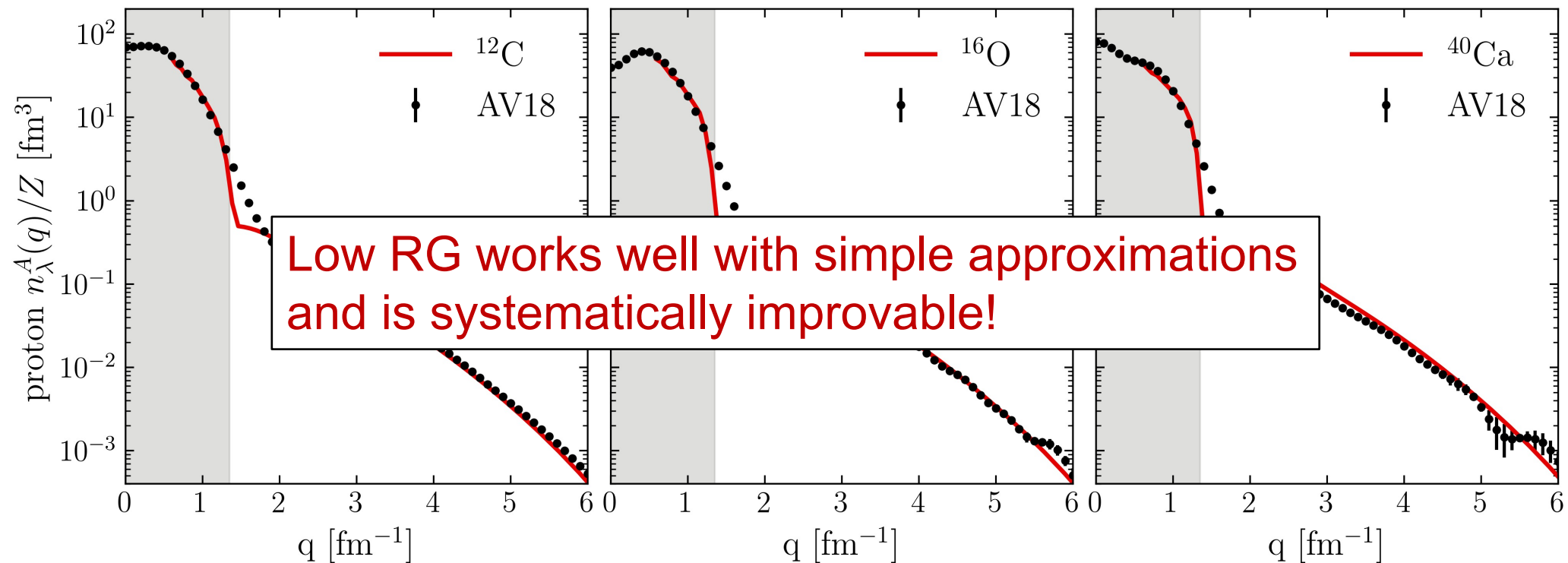
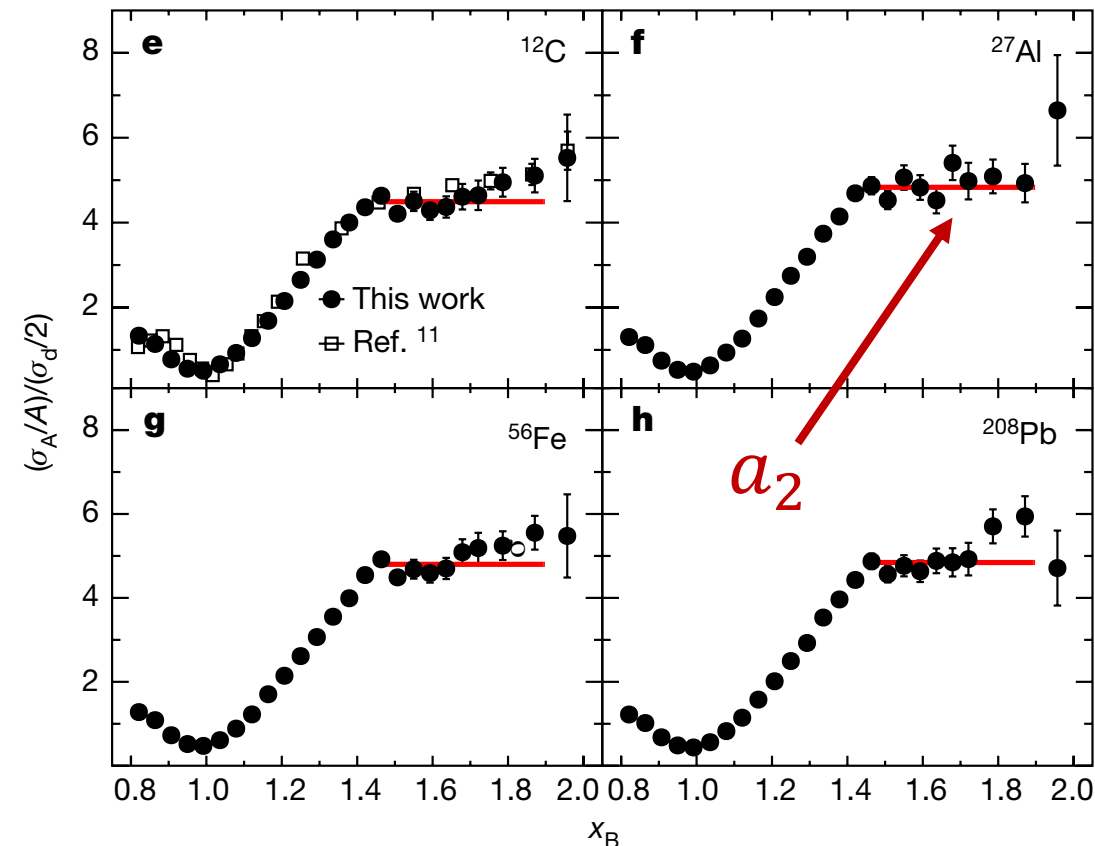


Fig. 3: Proton momentum distributions for ^{12}C , ^{16}O , and ^{40}Ca under LDA with AV18, $\lambda = 1.35 \text{ fm}^{-1}$, and densities from Skyrme EDF SLy4 using the HFBRAD code².

SRC scaling factors



- SRC scaling factors a_2 defined by plateau in cross section ratio $\frac{2\sigma_A}{A\sigma_d}$ at $1.45 \leq x \leq 1.9$

- Extract a_2 from momentum distributions

$$a_2 = \lim_{q \rightarrow \infty} \frac{P^A(q)}{P^d(q)} \approx \frac{\int_{\Delta p^{high}} dq P^A(q)}{\int_{\Delta p^{high}} dq P^d(q)}$$

where $P^A(q)$ is the single-nucleon probability distribution in nucleus A

Fig. 4: Ratio of per-nucleon electron scattering cross section of nucleus A to that of deuterium, where the red line indicates a constant fit. Figure from B. Schmookler et al. (CLAS), Nature **566**, 354 (2019).

SRC scaling factors

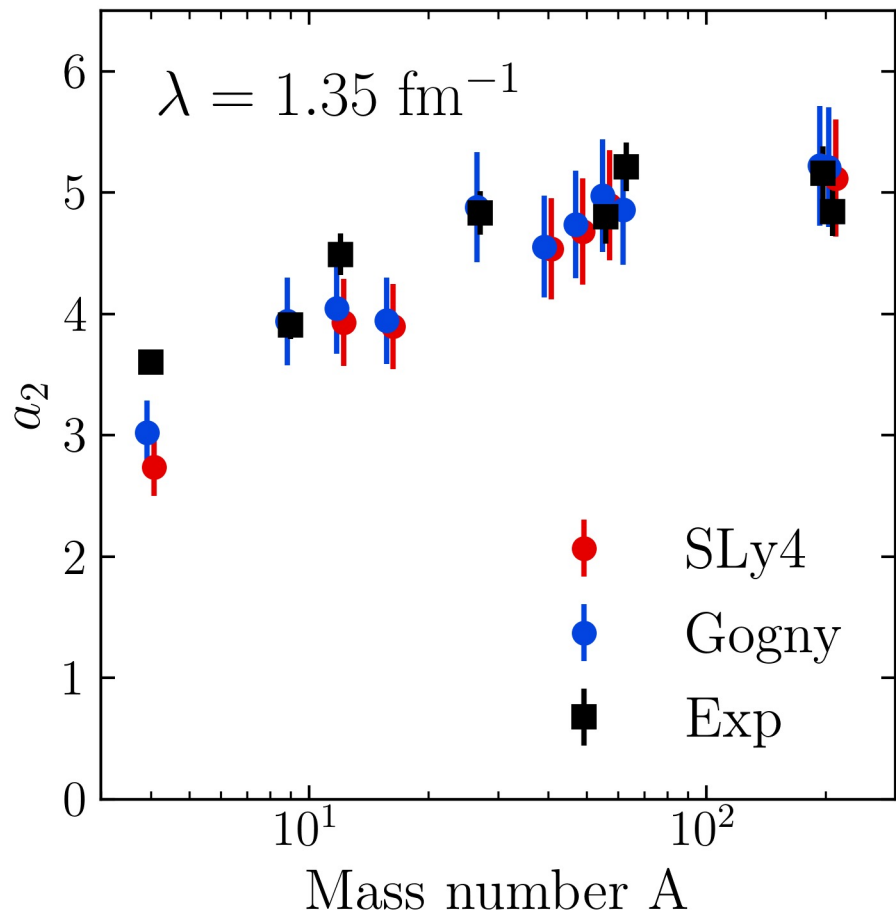


Fig. 5: a_2 scale factors using single-nucleon momentum distributions under LDA (SLy4 in red¹, Gogny² in blue) with AV18 and $\lambda = 1.35 \text{ fm}^{-1}$ compared to experimental values³.

- SRC scaling factors a_2 defined by plateau in cross section ratio $\frac{2\sigma_A}{A\sigma_d}$ at $1.45 \leq x \leq 1.9$
- Extract a_2 from momentum distributions

$$a_2 = \lim_{q \rightarrow \infty} \frac{P^A(q)}{P^d(q)} \approx \frac{\int_{\Delta p^{high}} dq P^A(q)}{\int_{\Delta p^{high}} dq P^d(q)}$$
 where $P^A(q)$ is the single-nucleon probability distribution in nucleus A
- Good agreement with a_2 values from experiment³ and LCA calculations⁴
- Error bars from varying Δp^{high}

SRC phenomenology

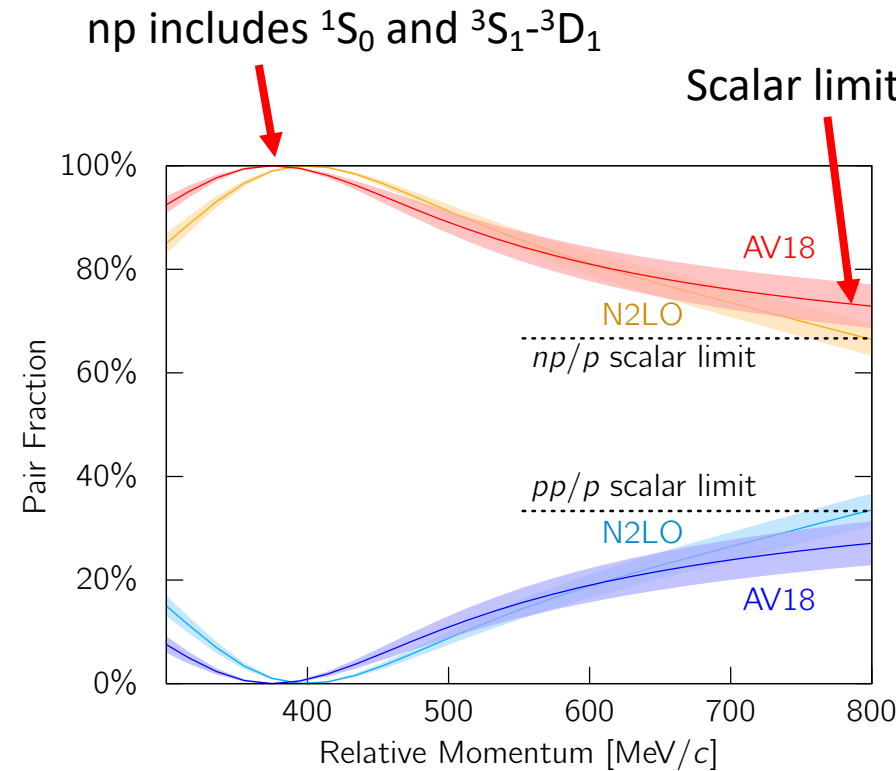
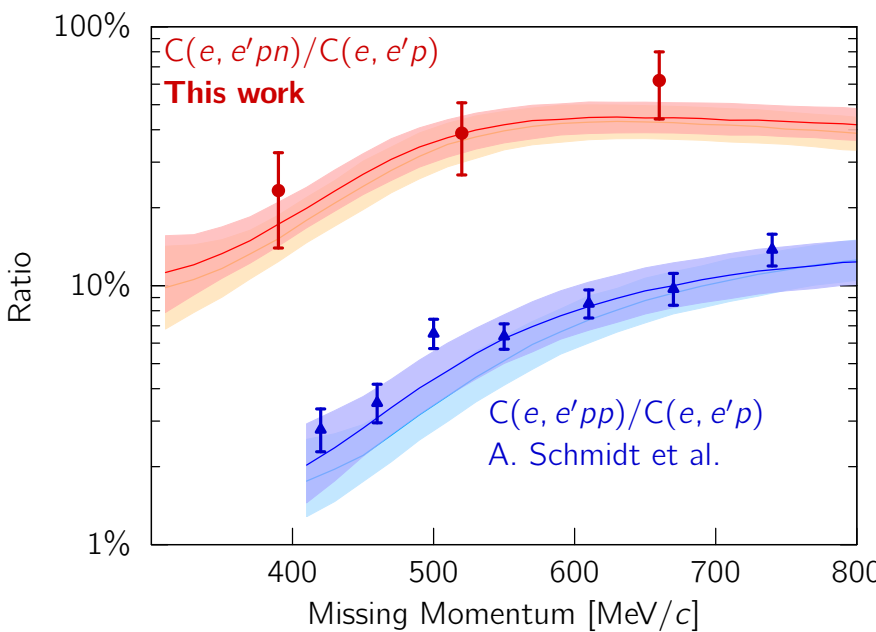
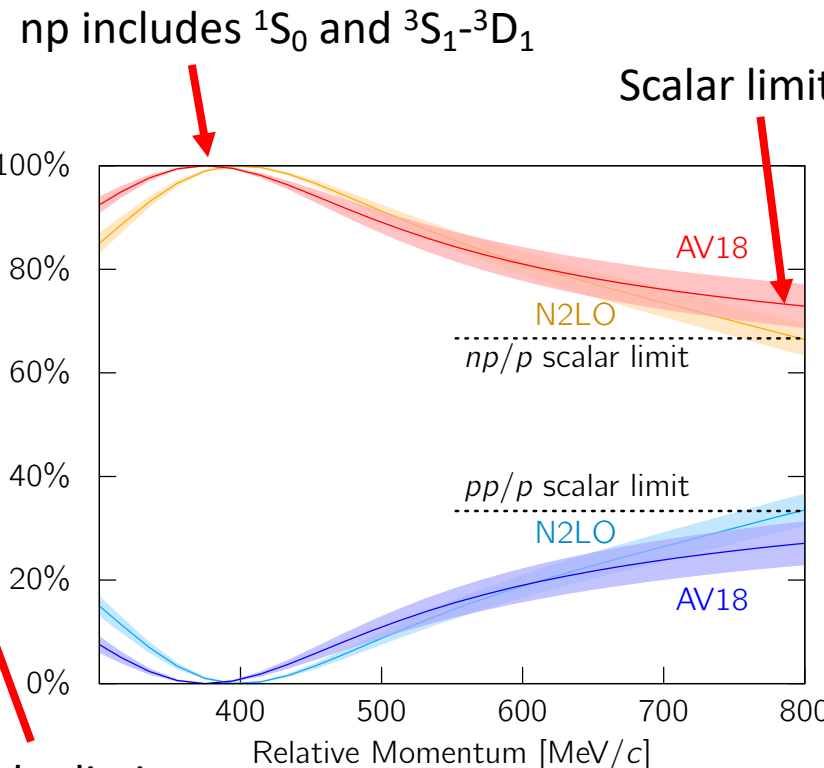
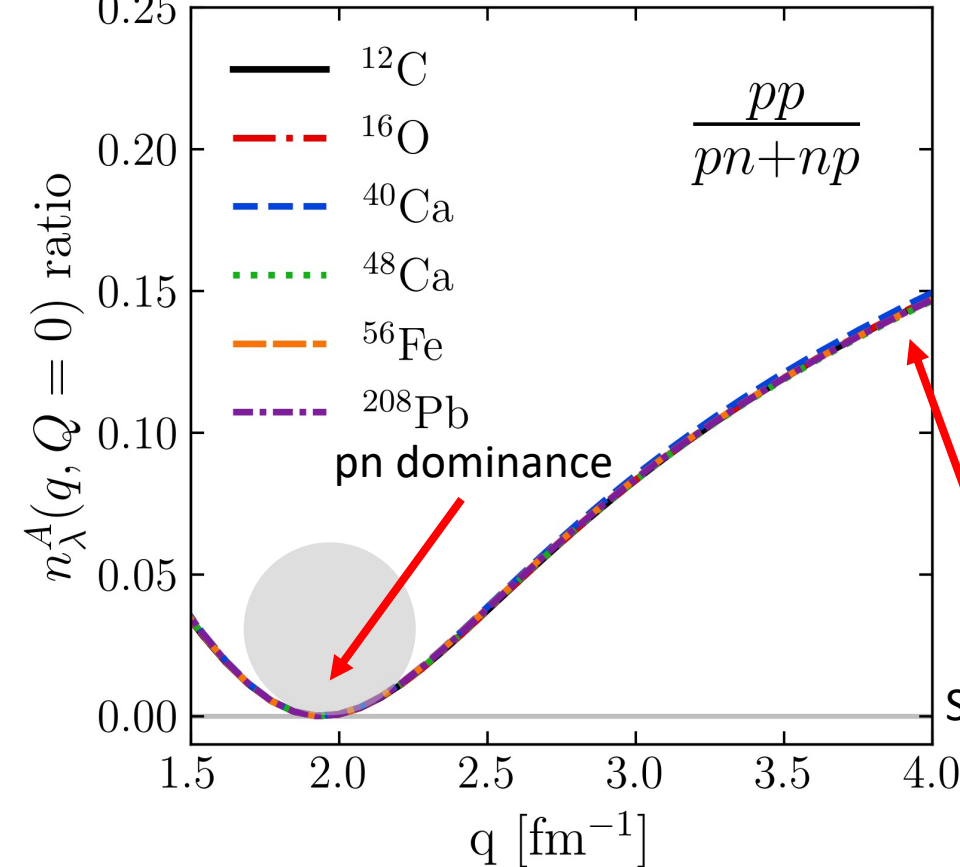


Fig. 6: (a) Ratio of two-nucleon to single-nucleon electron-scattering cross sections for carbon as a function of missing momentum. (b) Fraction of np to p and pp to p pairs versus the relative momentum. Figure from CLAS collaboration publication¹.

- At **high RG resolution**, the tensor force and the repulsive core of the NN interaction kicks nucleon pairs into SRCs
- np dominates because the tensor force requires spin triplet pairs (pp are spin singlets)
- **Do we describe this physics at low RG resolution?**

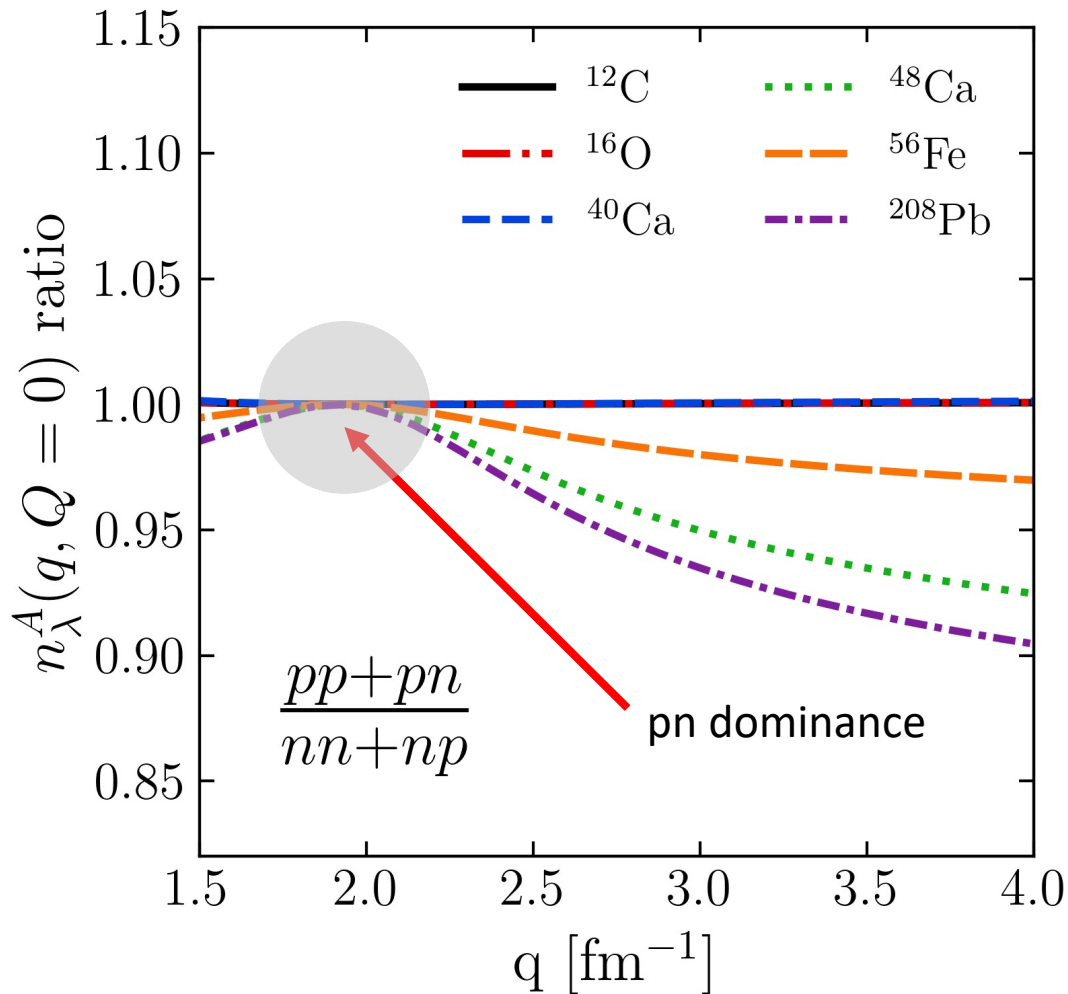
SRC phenomenology



- At low RG resolution, SRCs are suppressed in the wave function and shifted into the operator
- Physics is established in the 2-body system – **can apply to any nucleus!**
- **Low RG resolution** picture reproduces the characteristics of cross section ratios using simple approximations

Fig. 7: pp/pn ratio of pair momentum distributions under LDA with AV18 and $\lambda = 1.35 \text{ fm}^{-1}$.

SRC phenomenology



- Ratio ~ 1 independent of N/Z in pn dominant region
- Ratio < 1 for nuclei where $N > Z$ and outside pn dominant region

Fig. 8: $(\text{pp}+\text{pn})/(\text{nn}+\text{np})$ ratio of pair momentum distributions under LDA with AV18 and $\lambda = 1.35 \text{ fm}^{-1}$. Anthony Tropiano, APS DNP 2021 Meeting

Other exclusive knockout reactions

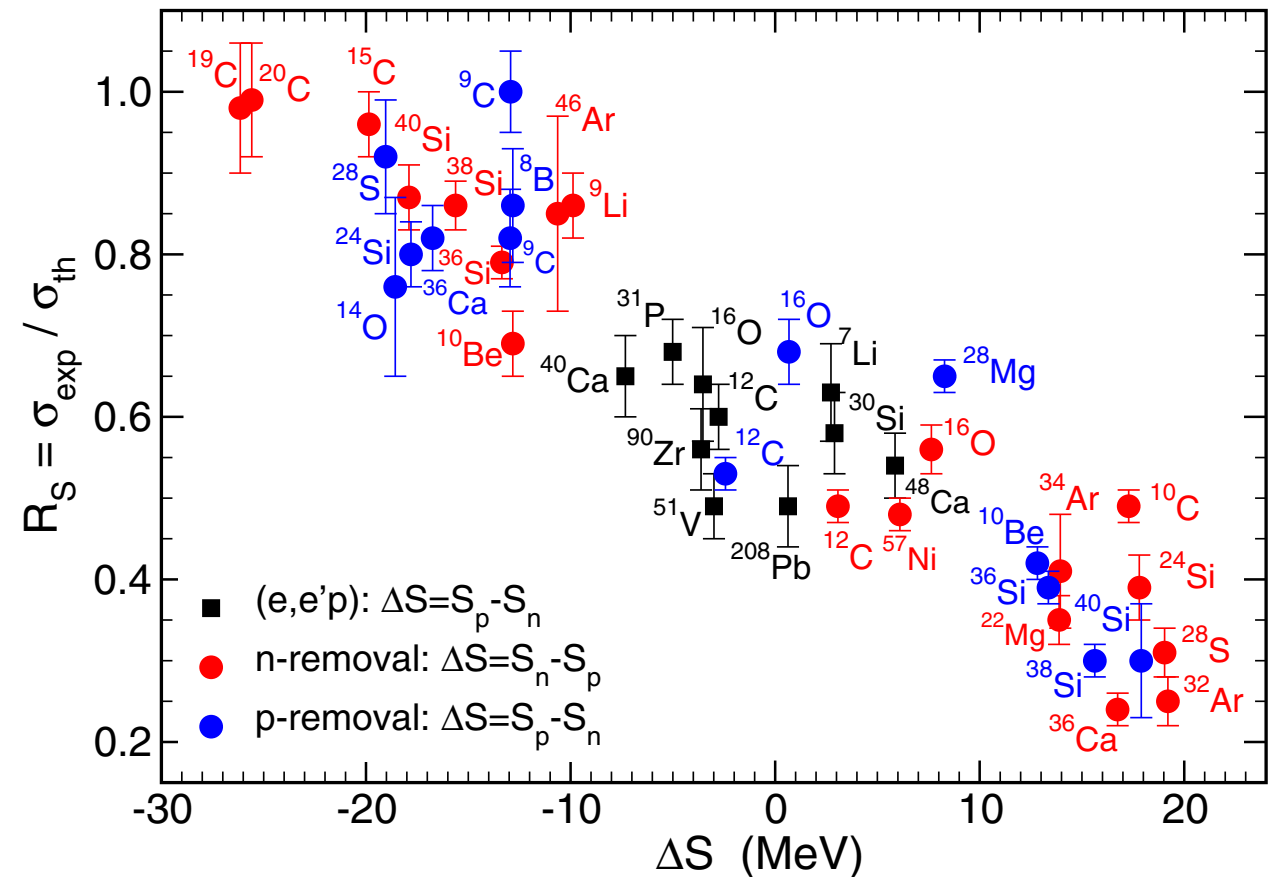


Fig. 9: R as a function of ΔS . Red (blue) points correspond to neutron-removal (proton-removal) cases. Solid black squares correspond to electron-induced proton knockout data. Figure from J. A. Tostevin and A. Gade, Phys. Rev. C **90**, 057602 (2014).

- RG analysis can help understand the cause of $R = \frac{\sigma_{exp}}{\sigma_{theory}} < 1$
- Mismatch of scale between one-body (**high RG**) operator and shell model structure (**low RG**) gives $\sigma_{theory} > \sigma_{exp}$

Other exclusive knockout reactions

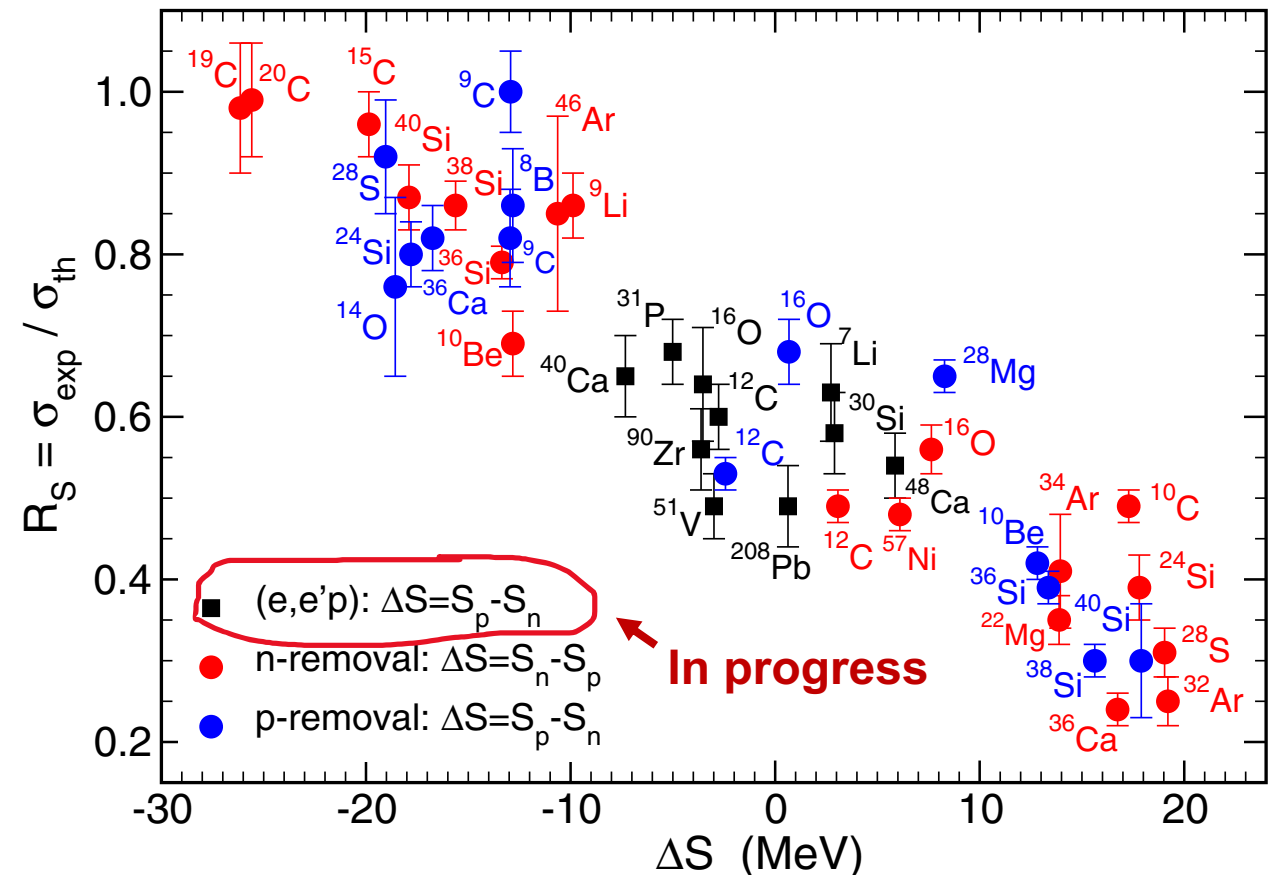


Fig. 9: R as a function of ΔS . Red (blue) points correspond to neutron-removal (proton-removal) cases. Solid black squares correspond to electron-induced proton knockout data. Figure from J. A. Tostevin and A. Gade, Phys. Rev. C **90**, 057602 (2014).

- RG analysis can help understand the cause of $R = \frac{\sigma_{\text{exp}}}{\sigma_{\text{theory}}} < 1$
- Mismatch of scale between one-body (**high RG**) operator and shell model structure (**low RG**) gives $\sigma_{\text{theory}} > \sigma_{\text{exp}}$
- Currently working on SRG-evolving spectroscopic factors for $(e, e'p)$ reactions

Summary and outlook

- Simple approximations work and are systematically improvable at low RG resolution
- Results suggest that we can analyze high-energy nuclear reactions using low RG resolution structure (e.g., shell model) and consistently evolved operators
 - Matching resolution scale between structure and reactions is crucial!
- Ongoing work:
 - Extend to cross sections and test scale/scheme dependence of extracted properties
 - Investigate impact of various corrections: 3-body terms, final state interactions, etc.
 - Apply to more complicated knock-out reactions (SRG with optical potentials)
 - Implement uncertainty quantification in low RG resolution calculations

Extras

Extras

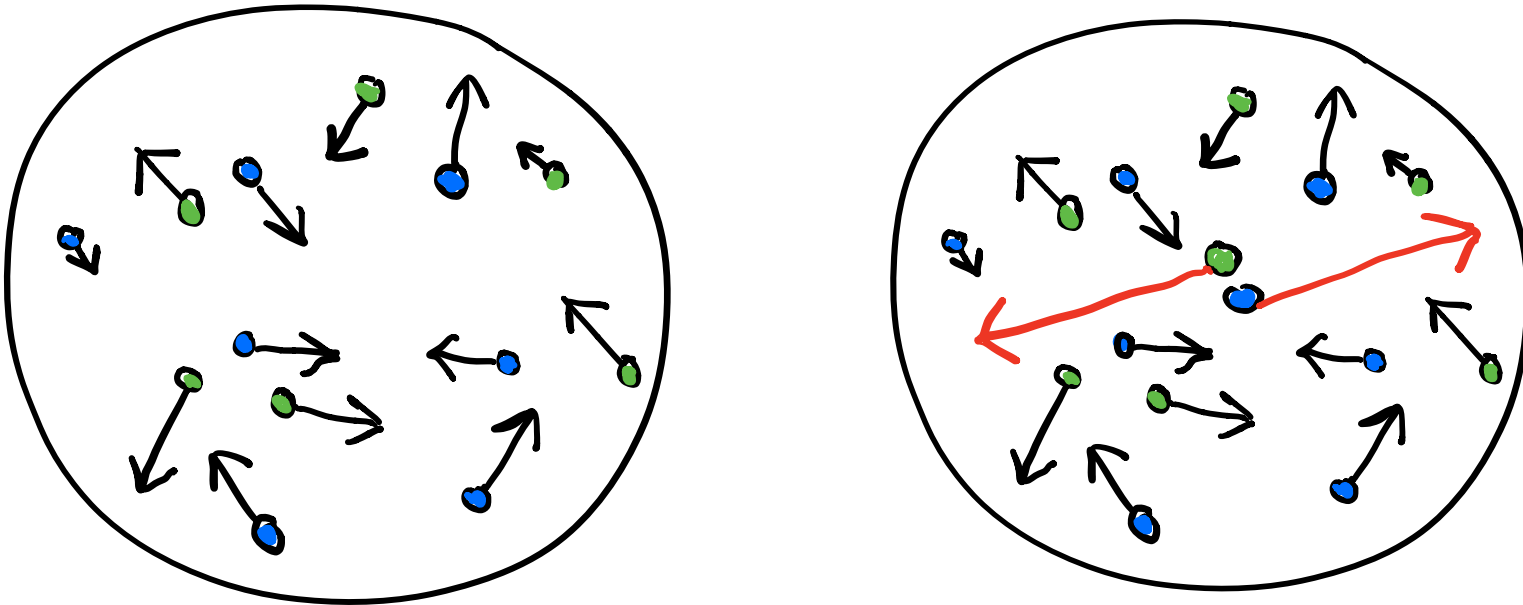


Fig. 10: Cartoon snapshots of a nucleus at (left) low-RG and (right) high-RG resolutions. The back-to-back nucleons at high-RG resolution are an SRC pair with small center-of-mass momentum.

SRG decoupling

- Evolve operators to low RG resolution

$$O(s) = U(s)O(0)U^\dagger(s)$$

where $s = 0 \rightarrow \infty$ and
 $U(s)$ is unitary

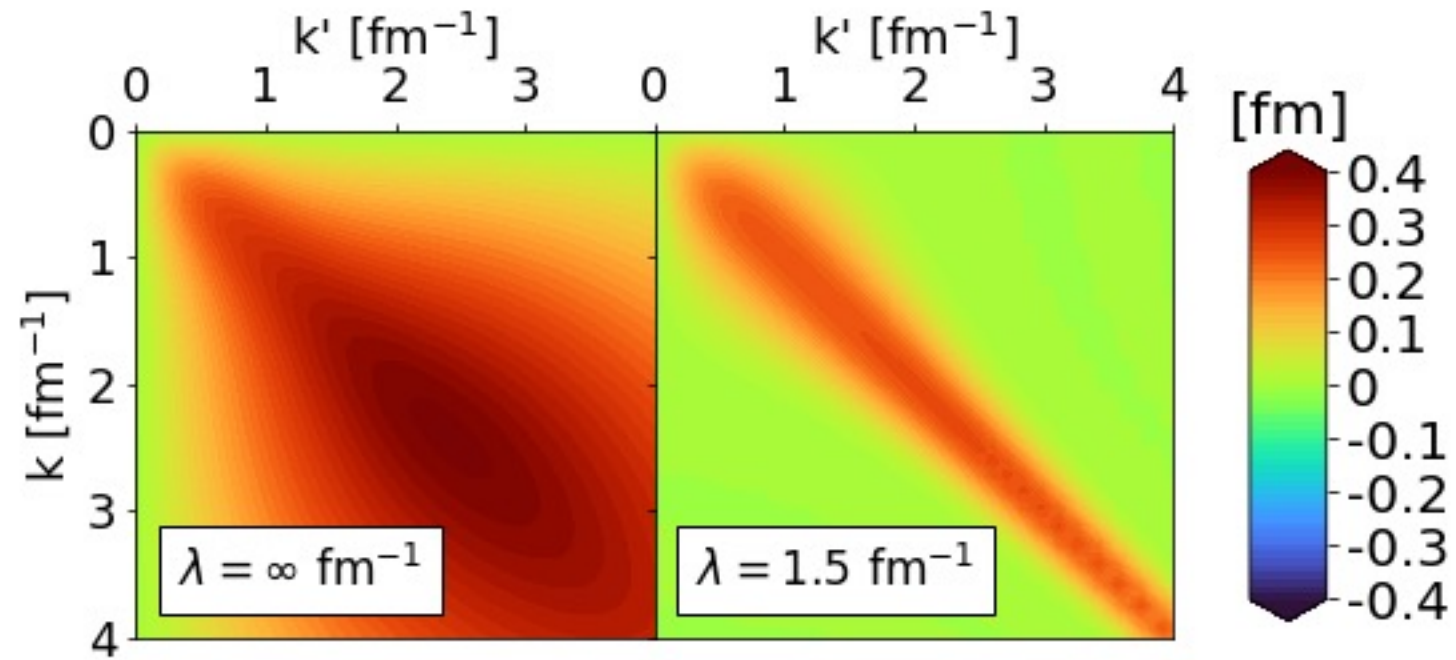


Fig. 11: Momentum space matrix elements of Argonne v18 (AV18) under SRG evolution in ${}^1\text{P}_1$ channel.

SRG decoupling

- Evolve operators to low RG resolution

$$O(s) = U(s)O(0)U^\dagger(s)$$

where $s = 0 \rightarrow \infty$ and $U(s)$ is unitary

- $\lambda = s^{-1/4}$ describes the decoupling scale of the RG evolved operator

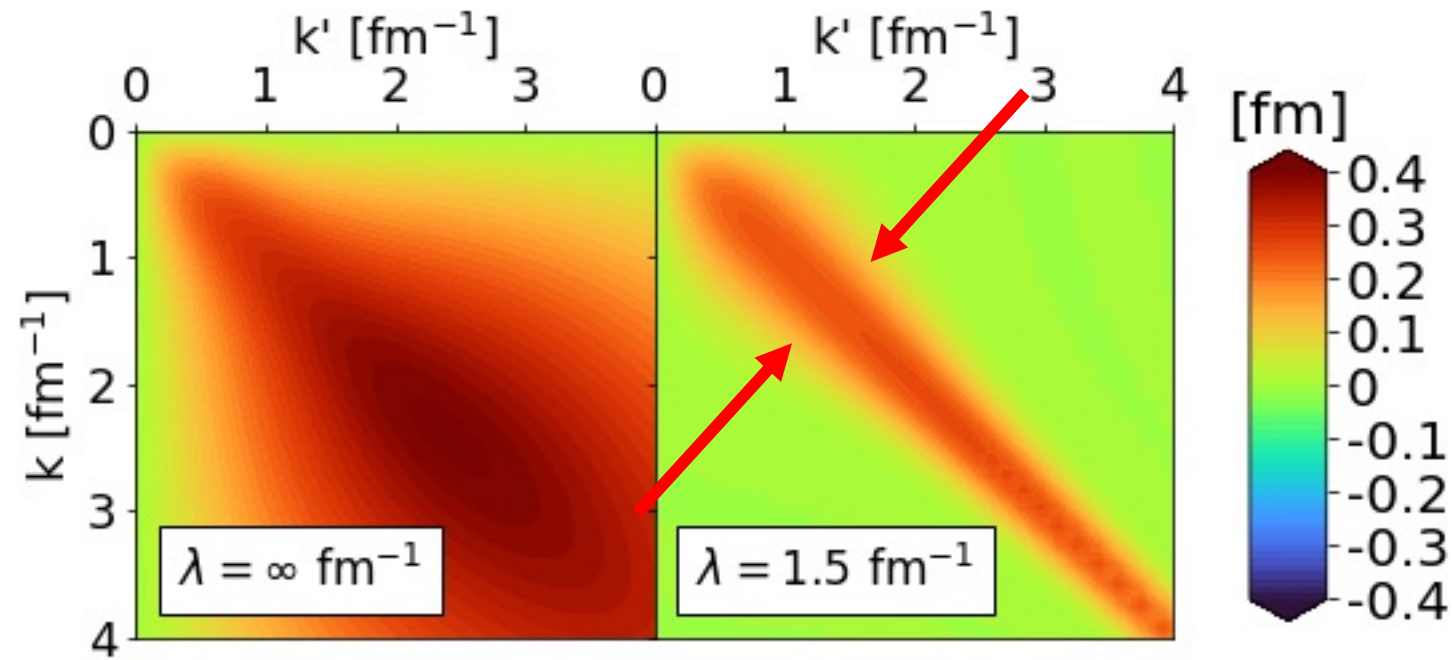


Fig. 11: Momentum space matrix elements of Argonne v18 (AV18) under SRG evolution in ${}^1\text{P}_1$ channel.

S-state and D-state contributions

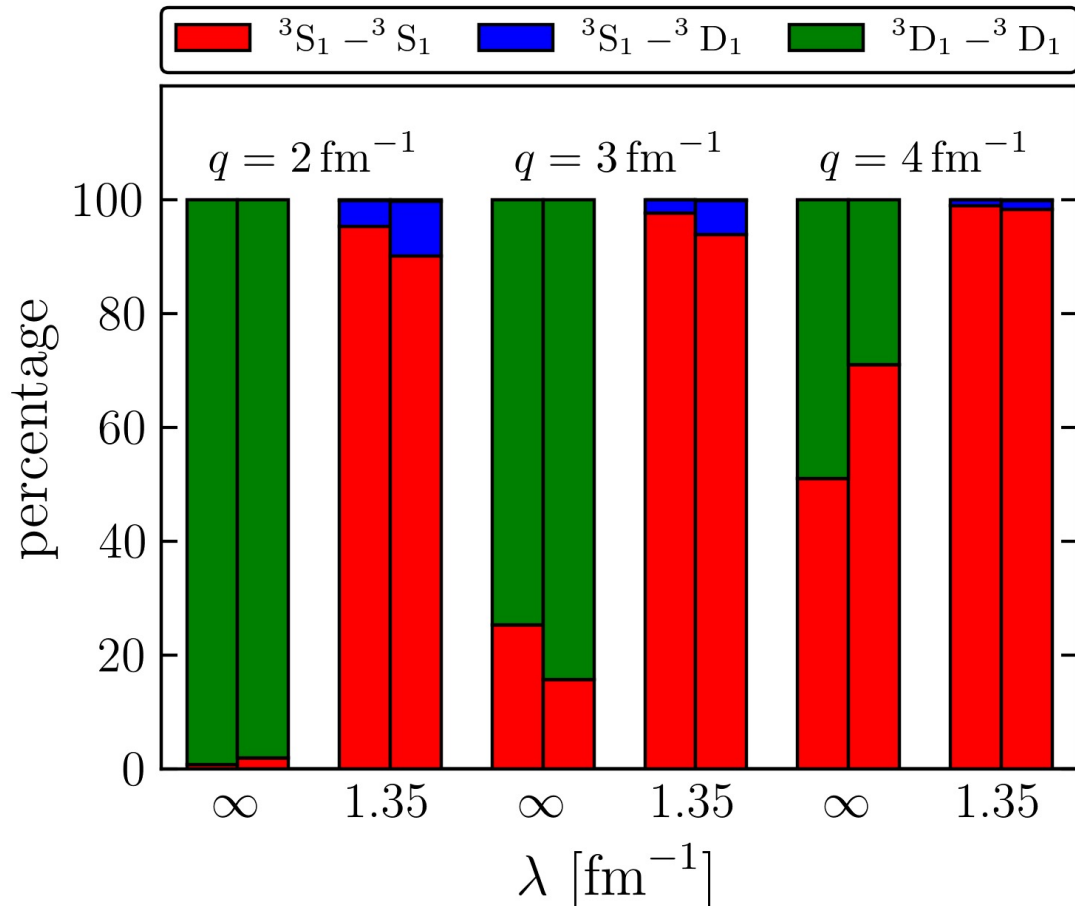
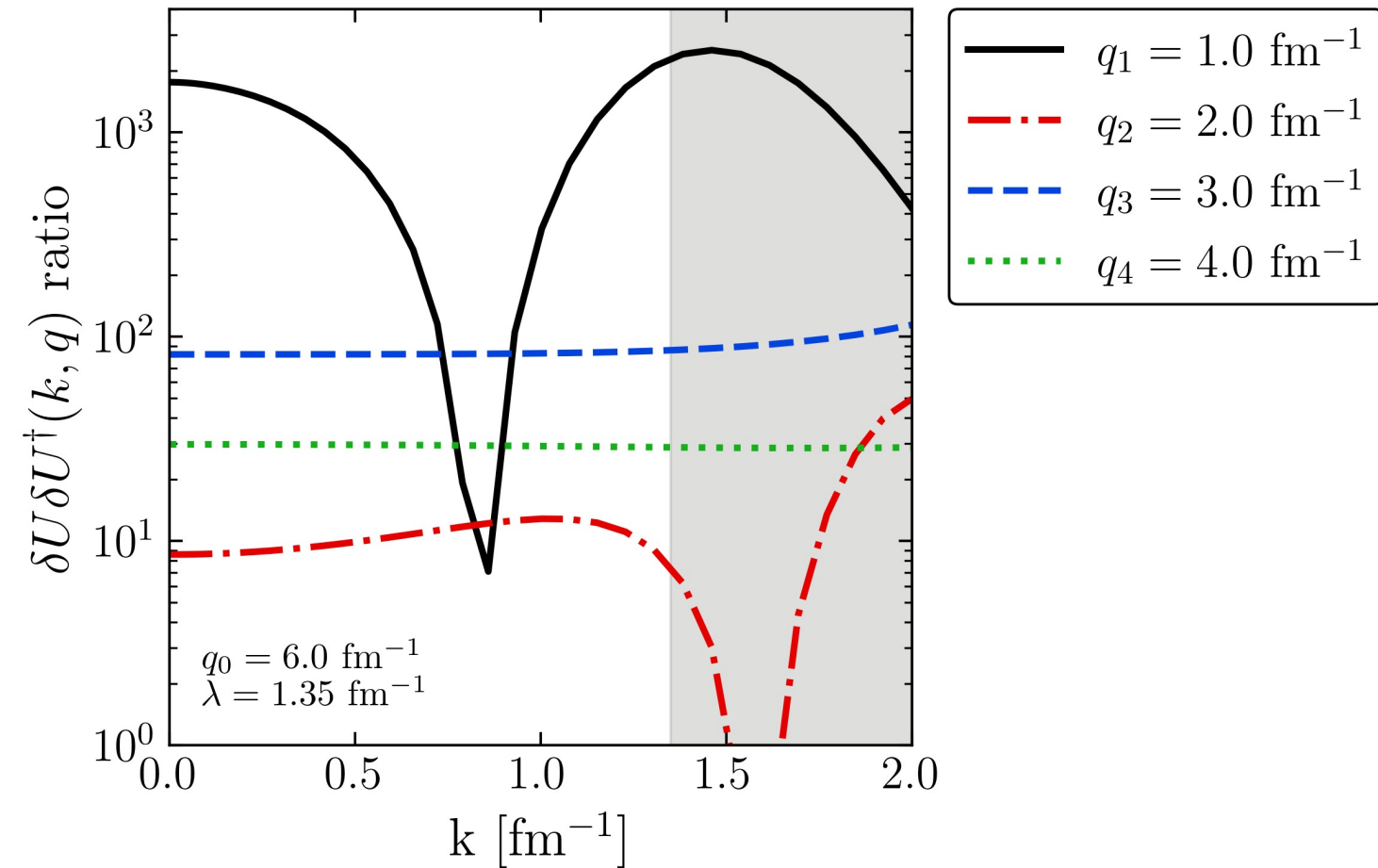
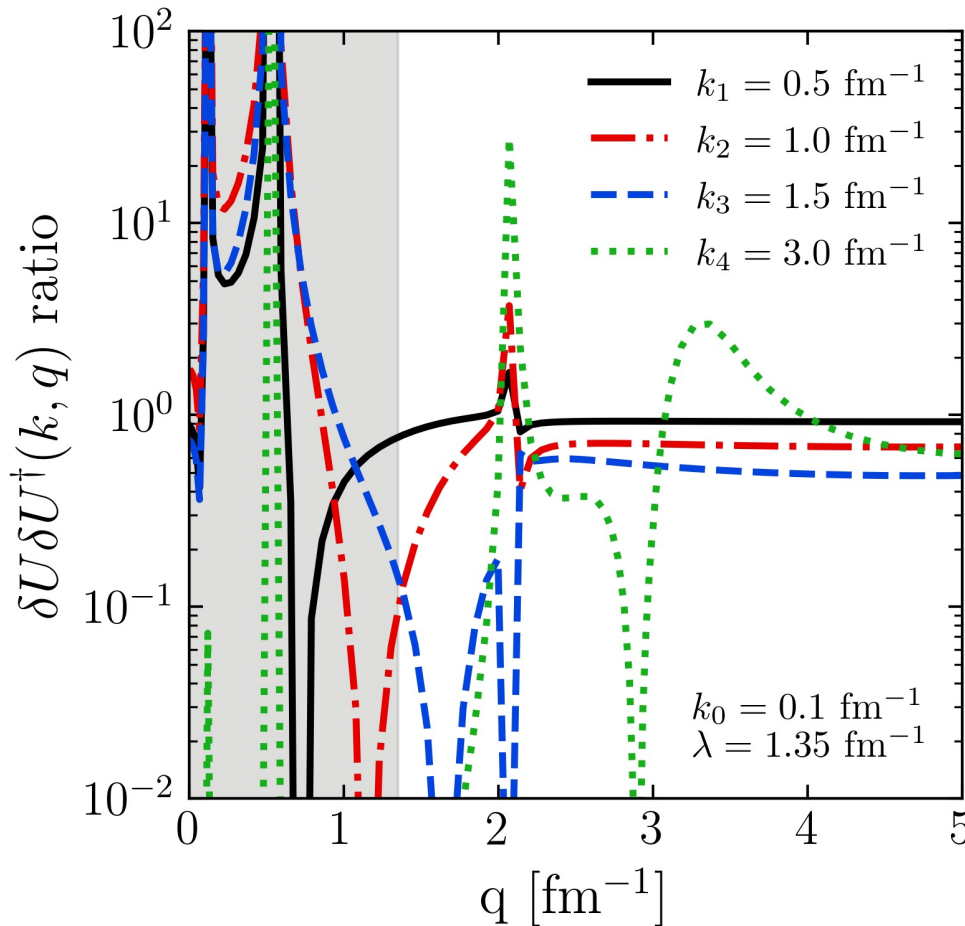


Fig. 12: Percentage contributions from each channel to the matrix element of the momentum distribution in the deuteron at several relative momentum values q for AV18 (left bar at each λ value) and Gezerlis N^2LO (right bar) potentials. We compare unevolved and SRG-evolved (both wave function and operator, so the net matrix element is unchanged) results where $\lambda = 1.35 \text{ fm}^{-1}$

Factorization



SRG λ dependence in momentum distributions

